Mitogen-activated protein kinase regulates neurofilament axonal transport

Walter Kong-Ho Chan[1,2], Angelo Dickerson[1,2], Daniela Ortiz[2], Aurea F. Pimenta[1,3], Catherine M. Moran[1,2], Jennifer Motil[1,2], Scotti J. Snyder[1,2], Kafaid Malik[4], Harish C. Pant[1,2,5] and Thomas B. Shea[1,2,*]

[1]Center Cell Neurobiology and Neurodegeneration Research and [2]Department of Biological Sciences, University of Massachusetts, Lowell, MA 01854, USA
[3]Department of Pharmacology, Vanderbilt University, Robinson Research Building, Nashville, TN 37232-8548, USA
[4]Department of Pharmacology, College of Medicine, University of Tennessee Center for Health Sciences, 874 Union Avenue, Memphis, TN 38163, USA
[5]Laboratory of Neurochemistry, NIH, NINDS, 36 Convent Drive, Bethesda, MD 20892, USA
*Author for correspondence (e-mail: thomas_shea@uml.edu)

Accepted 2 February 2004
Journal of Cell Science 117, 4629-4642 Published by The Company of Biologists 2004
doi:10.1242/jcs.01135

Summary

Mitogen-activated protein kinase (MAP) kinase plays a pivotal role in the development of the nervous system by mediating both neurogenesis and neuronal differentiation. Here we examined whether p42/44 MAP kinase plays a role in axonal transport and the organization of neurofilaments (NFs) in axonal neurites. Dominant-negative p42/44 MAP kinase, anti-MAP kinase antisense oligonucleotides and the MAP kinase inhibitor PD98059 all reduced NF phospho-epitopes and inhibited anterograde NF axonal transport of GFP-tagged NF subunits in differentiated NB2a/d1 neuroblastoma cells. Expression of constitutively active MAP kinase and intracellular delivery of active enzyme increased NF phospho-epitopes and increased NF axonal transport. Longer treatment with PD98059 shifted NF transport from anterograde to retrograde. PD98059 did not inhibit overall axonal transport nor compromise overall axonal architecture or composition. The p38 MAP kinase inhibitor SB202190 did not inhibit NF transport whereas the kinase inhibitor olomoucine inhibited both NF and mitochondrial transport. Axonal transport of NFs containing NF-H whose C-terminal region was mutated to mimic extensive phosphorylation was substantially less affected by PD98059 compared to a wild-type construct. These data suggest that p42/44 MAP kinase regulates NF anterograde transport by NF C-terminal phosphorylation. MAP kinase may therefore stabilize developing axons by promoting the accumulation of NFs within growing axonal neurites.

Key words: Mitogen-activated protein kinase, Neurofilaments, Axonal transport, Phosphorylation, Axonal maturation, Cytoskeleton, Signal transduction

Introduction

Mammalian neurofilaments (NFs), a major constituent of the axonal cytoskeleton, are 10 nm filaments composed of three polypeptide subunits, termed NF-H, NF-M and NF-L (for high, medium and low with respect to their molecular mass). NF subunits are among the most highly phosphorylated proteins in the nervous system (Hoffman and Lasek, 1975; Julien and Mushynski, 1983; Hoffman et al., 1984; Nixon et al., 1987). The C-terminal regions, or 'sidearms' of the subunits differ markedly from each other. Extensive phosphorylation of NF-H and NF-M C-terminal sidearms (that extend away from the filament backbone) initiates within cell bodies and continues during axonal transport, resulting in segregation of extensively phosphorylated NFs within axons. In contrast, hypophosphorylated NFs are largely confined to perikarya (for review, see Pant and Veeranna, 1995; Miller et al., 2002). Phosphorylation has long been considered to regulate several aspects of NF dynamics, including rendering subunits more resistant to proteolysis (Pant, 1988) increasing NF spacing and axonal caliber (Hirokawa et al., 1984; Nixon et al., 1994; Sanchez et al., 2000), dissociating NFs from the anterograde motor kinesin (Yabe et al., 1999), slowing of axonal transport rate (Jung and Shea, 1999; Jung and Shea, 2004; Jung et al., 2000a; Jung et al., 2000b; Lewis and Nixon, 1998; Zhu et al., 1998) and promoting NF-NF interactions leading to bundling within axons (Gou et al., 1998; Leterrier et al., 1996; Yabe et al., 2001a; Yabe et al., 2001b). However, the extent to which C-terminal NF phosphorylation contributes to some of these phenomena continues to be debated (Ackerley et al., 2003; Rao et al., 2002; Shea et al., 2003).

Kinases phosphorylating the C-terminal regions of NF-H and/or NF-M include glycogen synthase kinase (GSK)-3α and 3β, cyclin-dependent kinase-5 (cdk5), mitogen-activated protein (MAP) kinase, casein kinase I and II and stress-activated protein (SAP) kinases (Brownlees et al., 2000; Giasson and Mushynski, 1996; Giasson and Mushynski, 1997; Guidato et al., 1996; Li et al., 1999; O'Ferrall et al., 2000; Sharma et al., 1999; Sun et al., 1996; Veeranna et al., 1998) (for reviews, see Pant and Veeranna, 1995; Julien and Mushynski, 1998). These kinases phosphorylate NFs at sites distinct from each other (Guidato et al., 1996; Sun et al., 1996; Veeranna et al., 1998), leaving open the possibility that they could mediate separate aspects of NF dynamics.

MAP kinases consist of a family of kinases with diverse

effects on cellular proliferation, differentiation and degeneration (Cobb, 1999; Johnson and Lapadat, 2002). One member of this family, p42/44 MAP kinase, mediates multiple aspects of neuronal development including the elaboration of axons and dendrites (Abe et al., 2001; Obara et al., 2002; Valliant et al., 2002) and regulates axonal transport of some vesicular elements (Kholodenko, 2002). As the accumulation of phosphorylated NFs within axons is thought to represent a critical stage in axonal stabilization and maturation (Nixon and Shea, 1992), we examined here whether p42/44 MAP kinase played a role in axonal transport and organization of NFs in axonal neurites.

Materials and Methods

Cell culture

NB2a/d1 cells were cultured in DMEM (Sigma, St Louis, MO) containing 10% fetal bovine serum (Sigma) on dishes with a 1 mm hole drilled in the center and a coverslip sealed beneath the hole. To induce outgrowth of axonal neurites, cultures received 1 mM dibutyryl cyclic AMP (dbcAMP; Sigma) for 3 days (Jung et al., 1998; Yabe et al., 2001a; Yabe et al., 2001b).

Transfection

Cells treated with dbcAMP for 2 days were transfected with a construct that encodes rat NF-M fused with green fluorescent protein (GFP-M) (Yabe et al., 1999) or with constructs (generous gifts of Dr Chris Miller, Inst. Psychiatry, King's College, London) encoding normal NF-H conjugated to GFP (GFP-Hwt) and the identical NF-H construct in which serines in selected KSP domains had been mutated to aspartates ('GFP-Hasp') to mimic a permanently phosphorylated state (Ackerley et al., 2003). Additional neurons were co-transfected with a mixture of GFP-M and constructs encoding constitutively active and dominant-negative p42/44 MAP kinase (Li et al., 1999), or with a construct expressing human tau 40 conjugated to enhanced cyan fluorescent protein (eCFP-htau40; generous gift of Dr E. Mandelkow) (Stamer et al., 2002). Transfection was carried out using lipofectamine according to the manufacturer's instructions (Sigma). Briefly, constructs (2 μg) were resuspended in 100 μl serum-free DMEM, then combined with 8 μl lipofectamine that had been resuspended in 100 μl serum-free DMEM and allowed to equilibrate for 45 minutes at room temperature. An additional 800 μl of serum-free DMEM was added and this mixture was then added to cultures. After incubating cultures for 3.5 hours an additional 1 ml DMEM containing 10% fetal bovine serum (FBS) was added (without removing the DNA:lipofectamine mixture) and incubation continued for 24 hours, after which the medium was replaced with 2 ml fresh DMEM containing 10% FBS. Cultures were first viewed at this time, because prior studies (Yabe et al., 1999; Yabe et al., 2001a; Yabe et al., 2001b) demonstrated that 18-24 hours were required for transfected cells to accumulate sufficient GFP-M for visualization. Accordingly, transfected cells had been treated with dbcAMP for 3 days prior to viewing, at which time they have elaborated axonal neurites containing phosphorylated NFs (Shea et al., 1988; Shea et al., 1990; Shea and Beermann, 1994). Successfully transfected cells were localized by GFP fluorescence. The effectiveness of MAP kinase variants expressed following transfection with either of the above MAP kinase constructs was confirmed by immunoblot analysis of phospho-NFs (see Results).

For co-transfection, 2 μl each of constructs encoding GFP-M and one of the MAP kinases were combined in the initial mixture described above. Transfection rates under these conditions routinely exceed 80%. In co-transfection experiments utilizing GFP-M and MAP kinase vectors, we did not attempt to confirm whether or not individual neurons were transfected with both vectors. Rather, we scored all neurons expressing GFP-M in cultures that had been transfected with GFP-M alone, as well as in cultures transfected with a mixture of GFP-M and MAP kinase. It remains possible that some of the neurons in cultures exposed to a mixture of vectors were in fact not transfected with, or did not express, MAP kinase. As we only scored neurons expressing GFP-M, we nevertheless remain confident of our results, as scoring neurons expressing GFP-M but not MAP kinase would cause us to underestimate the impact of alteration of MAP kinase activity on the distribution of GFP-M. Our transfection results presented here, although statistically significant, therefore are likely to underestimate the full effect of MAP kinase on NF axonal transport and organization. GFP-labeled structures exist in multiple forms in both NB2a/d1 cells and primary neurons, including those that are apparently filamentous, as well as punctate structures (e.g. Wang and Brown, 2001; Yabe et al., 1999; Yabe et al., 2001a; Yabe et al., 2001b), which in some instances may represent coiled filaments (Wang and Brown, 2001). In images where all or most of the GFP-labeled profiles are not clearly filamentous, we refer to them as 'NF subunits' solely to avoid arbitrarily designating assembly into a filamentous form. This is not necessarily intended to indicate transport as non-filamentous oligomers or individual subunits (e.g. Yabe et al., 1999).

Antisense and sense oligonucleotide treatment

Cells treated with dbcAMP for 2 days were incubated for the final 24 hours of dbcAMP treatment with 10 μM oligonucleotides corresponding to the sequence for p42/44 MAP kinase in sense and antisense orientation. These oligonucleotides have previously been demonstrated to decrease MAP kinase levels and activity in cultured neuroblastoma (Ekinci et al., 1999). Oligonucleotides were added to GFP-M transfected cells immediately after transfection. Efficacy of antisense oligonucleotides was confirmed here by decreased MAP kinase levels in immunoblot analyses and alteration of NF phosphorylation.

Intracellular delivery of MAP kinase

Purified active MAP kinase (UBI, Lake Placid, NY) was delivered via the commercial Provectin delivery system (Imgenex, San Diego, CA) into cells that had been differentiated for 2 days with dbcAMP, and MAP kinase levels were examined 24 hours later (i.e., after a total of 3 days of dbcAMP treatment). For cells transfected with GFP-M, Provectin-mediated intracellular delivery of MAP kinase was carried out immediately after transfection. MAP kinase (final concentration 1 mg/ml) was mixed with the resuspended Provectin reagent in HEPES buffer for 5 minutes then added to cultures for 4 hours, after which medium was changed according to the manufacturer's instructions and cultures were viewed under phase-contrast and UV optics. In additional experiments, MAP kinase was heat-inactivated by boiling for 5 minutes prior to mixing with Provectin. The efficacy of Provectin-mediated intracellular delivery of protein was confirmed by intracellular delivery of β-galactosidase followed by histochemical analyses for β-galactosidase activity (provided as a positive control by the manufacturer). Efficacy of Provectin-mediated delivery of active MAP kinase was also confirmed by increased MAP kinase in immunoblot analyses and alteration of NF phosphorylation (see Results). As with double transfections, we did not ascertain whether individual cells expressed GFP-M and received detectable MAP kinase following sequential transfection and Provectin treatment; however, the high rates of transfection and intracellular delivery via Provectin suggest that most cells received both GFP-M and MAP kinase. Moreover, this is supported by our results (below), which demonstrate clear differences in transport of GFP-M following intracellular delivery of active MAP kinase.

Treatment with pharmacological inhibitors

Cultures were treated with 10 μM PD98059, an inhibitor of MEK, the upstream activator of p42/44 MAP kinase and 10 μM SB202190 (each from Calbiochem, La Jolla, CA), which inhibits p38 MAP kinase (Alessi et al., 1995; Cuenda et al., 1995; Manthey et al., 1998; Pang et al., 1995). As an additional control, some cultures were treated with 5 μM olomoucine (Sigma), which is reported to inhibit anterograde axonal transport (Ratner et al., 1998). Inhibitors were added for the final 2 hours of incubation following transfection.

Immunoblot analysis and immunofluorescence

For immunoblot analysis, cultures were rinsed with Tris-buffered saline (TBS) (pH 7.4), then homogenized in 1% Triton in 0.5M Tris (pH 6.8) containing 5 mM EDTA, 1 mM PMSF and 50 μg/ml leupeptin (Jung et al., 1998). Samples received an equal volume of 2× Laemmli treatment buffer, were boiled for 1 minute and electrophoresed on linear 7% polyacrylamide SDS gels. Separated proteins were transferred to nitrocellulose and were probed as described (Shea et al., 1997) with 1:1000 dilutions of monoclonal antibodies (SMI-31, RT97) directed against phospho-epitopes of NF-H and NF-M, and a polyclonal antibody (L3) generated against electrophoretically purified NF-L, followed by goat anti-mouse IgG conjugated to alkaline phosphatase as described previously (Jung et al., 1998). [SM1-31 was obtained from Sternberger Meyer Monoclonals, Lutherville, MD; RT97 was a generous gift of B. Anderton, Institute of Psychiatry, London, UK; anti-NF-L was raised in this laboratory (see Jung et al., 1998); anti-MAP kinase was obtained from UBI, Lake Placid, NY.]

For immunofluorescence, cultures were fixed with 4% paraformaldehyde in TBS for 5 minutes at room temperature. The cultures were then rinsed twice for 5 minutes in TBS, blocked for 30 minutes in TBS containing 1% bovine serum albumin (BSA) and 2% normal goat serum and incubated overnight at 4°C in TBS containing 1% BSA and 1:100 dilutions of RT97, L3, a polyclonal antibody directed against beta-tubulin (Sigma) and monoclonal antibodies directed against phosphorylated (PHF-1) (Greenburg and Davies, 1990), nonphosphorylated (Tau-1) (Kosik et al., 1989) and phospho-independent (5E2) (Joachim et al., 1987) epitopes of tau. The following morning, cultures were rinsed three times with TBS, re-blocked for 30 minutes, rinsed with TBS, then incubated for 30 minutes at 37°C in TBS containing 1% BSA and a 1:150 dilution of Texas Red conjugated goat anti-rabbit IgG. Cells were rinsed three times with TBS and stored at 4°C. Filamentous actin was visualized by staining with rhodamine-phalloidin (Molecular Probes, Inc.). Cultures were rinsed twice with PBS and fixed as described above. Samples were rinsed again with PBS, extracted for 5 minutes with –20ºC acetone and air-dried. Rhodamine-phalloidin was dissolved in methanol, evaporated to dryness, then re-dissolved in 400 μl PBS according to the manufacturer's instructions. Cultures were incubated with this solution for 20 minutes at 25°C, rinsed twice with PBS and stored in PBS at 4°C in the dark until visualization. Additional transfected cultures and cultures treated with oligonucleotides and pharmacological inhibitors were stained without fixation with 40 mM Mitotracker (Molecular Probes) to monitor transport of vesicular elements (e.g. Trinzcek et al., 1999).

Image acquisition and densitometric analysis

Epifluorescent and corresponding phase-contrast images were captured with a DAGE CCL-72 camera via NIH Image software (available as freeware from http://rsb.info.nih.gov/nih-image) using a Scion LG-3 frame grabber or via a Photometrics Coolsnap camera operated by OpenLab software (Improvision). Images were stored as TIFF or PICT files and analyzed using NIH Image software as described (Jung et al., 1998). Briefly, densitometric analyses were carried out by encircling cells or axonal neurites with the freehand selection tool. Images were inverted and background was subtracted using the automated function. For calculation of relative density along axonal neurites, individual axonal neurites were divided into thirds. Axonal neurites were scored as possessing filamentous GFP within their distal-most third if both a signal greater than 10% above background was obtained and GFP was predominantly associated with the central bundle (Yabe et al., 2001a; Yabe et al., 2001b). Relative density of immunoreactive proteins in immunoblot analyses was also determined by encircling bands with the freehand tool on digitized images of immunoblots. Values obtained from multiple cells and blots were exported into Microsoft Excel for calculation of ratios and statistical analyses.

For real-time analysis of axonal transport of GFP-labeled structures, digital images of transfected cells were captured at intervals before and after treatment with pharmacological agents. Translocation of GFP-labeled structures was measured on digital images using an arbitrary vertical line drawn across the identical location in sequential images; particles were considered to have undergone net translocation provided that they translocated at least one full respective particle length (Yabe et al., 1999).

Results

Manipulation of MAP kinase levels in cells

In order to probe the effects of MAP kinase activity on intracellular NF dynamics, we aimed to up- and down-regulate levels of MAP kinase in several ways, including incubation of cells with antisense- and sense-oriented oligonucleotides directed against MAP kinase (Ekinci et al., 1999), constructs expressing constitutively active and dominant-negative forms of MAP kinase (Li et al., 1999) and Provectin-mediated intracellular delivery of active and inactive MAP kinase. Immunoblot analysis of cytosolic extracts from cells treated with antisense oligonucleotides for 24 hours demonstrated a reduction in MAP kinase levels (Fig. 1). We also attempted to upregulate MAP kinase levels by intracellular delivery of active MAP kinase via the Provectin delivery system. The efficacy of Provectin-mediated intracellular delivery of protein into dbcAMP-treated NB2a/d1 cells was first examined by intracellular delivery of β-galactosidase followed by histochemical analysis for β-galactosidase activity. All cells (100%) expressed β-galactosidase activity following incubation with Provectin mixed with β-galactosidase, whereas none expressed activity following incubation with Provectin alone or with β-galactosidase in the absence of Provectin (Fig. 1A). As these data confirmed the efficacy of Provectin-mediated intracellular delivery, we next incubated cells under the same conditions with purified MAP kinase; intracellular delivery of MAP kinase via Provectin was confirmed by an approximate 35% increase in MAP kinase levels in immunoblot analysis (Fig. 1B). Immunoblot analyses also confirmed that treatment with antisense oligonucleotide reduced MAP kinase levels by nearly 40% (Fig. 1B).

MAP kinase alters intracellular NF phosphorylation

As MAP kinase has been reported to phosphorylate NF subunits (Veeranna et al., 1998), we next examined the effects of the above alterations in MAP kinase levels on NF phosphorylation in differentiated NB2a/d1 cells. Immunoblotting of Triton-insoluble cytoskeletons with antibodies to NF phospho-epitopes demonstrated that reduction of MAP kinase by each of several methods reduced

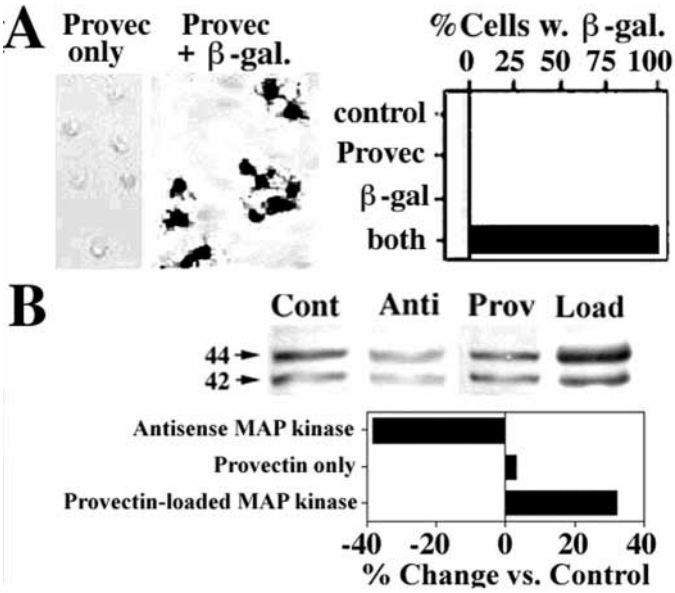

Fig. 1. Alteration of MAP kinase levels in NB2a/d1 cells. (A) Cultures were treated with either Provectin or β-galactosidase or both together, followed by histochemical analysis for β-galactosidase. Bright-field images of cells exposed for 4 hours to Provectin alone (Provec) or Provectin mixed with β-galactosidase (Provec + β-gal) are shown. The accompanying graph depicts the percentage of cells expressing β-galactosidase activity in multiple fields of duplicate cultures; 100% of cells expressed β-galactosidase activity following incubation with Provectin and β-galactosidase, whereas 0% expressed activity following incubation with Provectin alone or with β-galactosidase in the absence of Provectin. (B) Immunoblot analysis of homogenates of control cultures (Cont) and cultures treated for 4 hours with Provectin (Prov) and Provectin loaded with purified MAP kinase (Load), or for 24 hours with antisense oligonucleotides directed against MAP kinase (Anti) as described in Materials and Methods. Anti-MAP kinase recognizes two bands of 44 and 42 kDa. The accompanying graph presents densitometric analyses of immunoblots treated as indicated prior to harvest; note that treatment with Provectin and MAP kinase increased MAP kinase levels by approximately 35%, whereas treatment with antisense oligonucleotides reduced MAP kinase levels by nearly 40%.

NF phospho-epitopes, whereas increasing active MAP kinase also increased NF phospho-epitopes. Treatment of cultures with a pharmacological inhibitor (PD98059) that prevents MAP kinase activation by MEK1-mediated phosphorylation (Alessi et al., 1995; Pang et al., 1995) reduced NF phospho-epitopes (Fig. 2). Treatment with antisense but not sense oligonucleotides also reduced NF phospho-epitopes (Fig. 2). Transfection with the above construct expressing dominant-negative MAP kinase reduced NF phospho-epitopes, whereas transfection with the above construct expressing constitutively

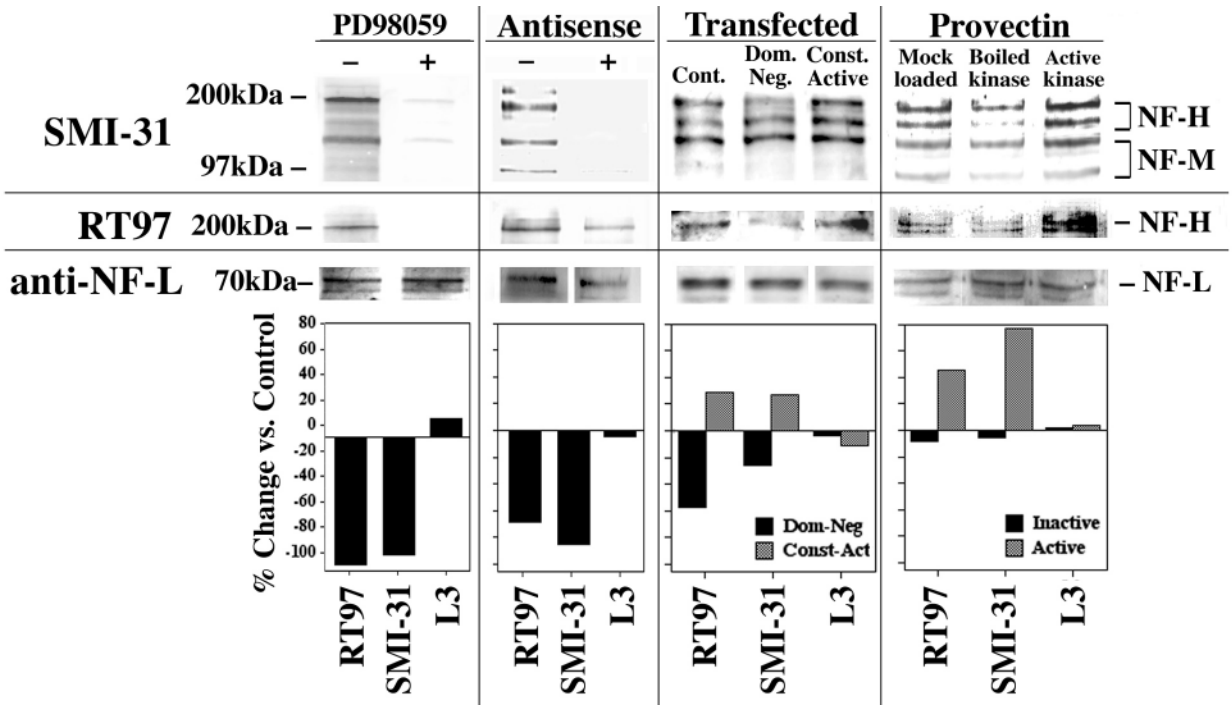

Fig. 2. MAP kinase alters intracellular NF phosphorylation. Immunoblot analyses of Triton-insoluble cytoskeletons from differentiated NB2a/d1 cells probed with SMI-31, RT97 and L3 (anti NF-L). Cells were immunoblotted following treatment with PD98059 (a MAP kinase activation inhibitor) (+, with PD98059; –, control); antisense (+) and sense (–) MAP kinase oligonucleotides; transfection with constructs expressing constitutively active and dominant-negative MAP kinase or following Provectin-mediated delivery of active or boiled MAP kinase or mock loaded as a control. Migratory positions of NF-H, NF-M and NF-L are indicated. The accompanying graphs present densitometric analyses, with values obtained from treated cultures expressed as % change compared to untreated cultures from the same experiment. Note that PD98059, antisense oligonucleotides and the dominant-negative MAP kinase decreased NF phospho-epitopes, whereas the constitutively active MAP kinase and intracellular delivery of active but not boiled MAP kinase increased NF phospho-epitopes. Note also that none of these treatments altered levels of NF-L immunoreactivity.

active MAP kinase increased NF phospho-epitopes (Fig. 2). Finally, intracellular delivery of active, but not inactive (boiled), MAP kinase increased NF phospho-epitopes (Fig. 2). Reprobing of the above immunoblots with a polyclonal antibody (L3) directed against NF-L revealed no change in NF-L levels following up- and down-regulation of MAP kinase activity, indicating that the above manipulations of MAP kinase activity induced alterations in NF phosphorylation state rather than total NF levels (Fig. 2).

MAP kinase affects NF dynamics

To examine whether alteration in MAP kinase activity affected NF dynamics, we transfected differentiated NB2a/d1 cells with a construct expressing NF-M conjugated to GFP (GFP-M) (Yabe et al., 1999; Yabe et al., 2001a; Yabe et al., 2001b) and monitored the distribution and organization of GFP-tagged NF subunits within axonal neurites following up- and down-regulation of MAP kinase activity by the above methods. Most neurites of cells differentiated and transfected as described in Materials and Methods exhibit a prominent NF bundle that has incorporated substantial GFP labeling along its length (Fig. 3A) (see also Yabe et al., 2001a; Yabe et al., 2001b). We therefore quantified the percentage of axonal neurites in which the NF bundle was labeled with GFP within the distal third of their length following up- and down-regulation of MAP kinase. This percentage was reduced following a 2-hour treatment with PD98059 (but not with its carrier, DMSO), treatment with antisense but not sense oligonucleotides corresponding to the sequence for MAP kinase and expression of dominant-negative MAP kinase (Fig. 3B,C). By contrast, this percentage was increased following Provectin-mediated intracellular delivery of active MAP kinase and by expression of constitutively active MAP kinase (Fig. 3C). Treatment with PD98059 did not prevent the increase in GFP-labeling of the central bundle induced by constitutively active MAP kinase (Fig. 3C). As the constitutively active kinase does not require phosphorylation for activity, this latter result therefore served as an additional control for the specificity of PD98059, as well as the constitutive activity of this construct (Li et al., 1999; Veeranna et al., 1998). Treatment with SB202190 did not alter the percentage of axonal neurites with GFP labeling within the distal axonal bundle (Fig. 3C), suggesting that, as observed for NF phosphorylation, p42/44 MAP kinase and not p38 MAP kinase, regulates NF dynamics within NB2a/d1 axonal neurites.

In addition to the large bundle that predominates along axonal neurites, endogenous NF subunits and subunits expressed following microinjection or transfection exist in multiple forms, including small filaments and non-filamentous punctate structures, both of which incorporate into the centrally situated NF bundle over time in a proximal to distal manner (Yabe et al., 2001a; Yabe et al., 2001b). As the possibility existed that manipulation of MAP kinase activity could have altered incorporation of subunits into the central bundle rather than overall transport, we also quantified total GFP fluorescence within the central and distal thirds of axonal neurites regardless of whether or not it was associated with the

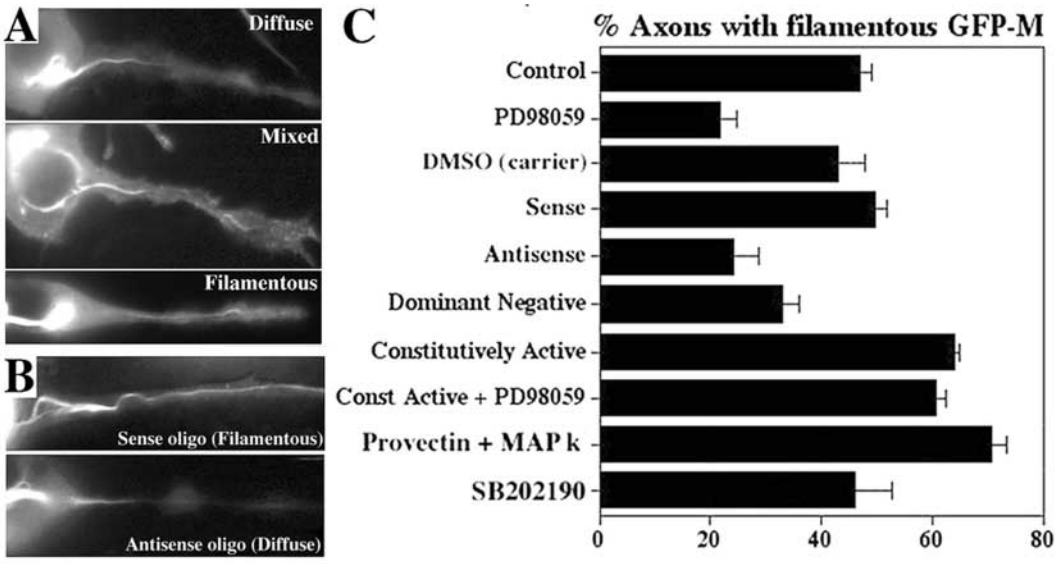

Fig. 3. MAP kinase inhibits accumulation of NFs in axonal neuritis. (A) Representative images of the various forms in which GFP-M is detected 24 hours after transfection of NB2a/d1 cells that had received dbcAMP for 2 days prior to transfection. As shown previously (Yabe et al., 2001b), most axonal neurites under these conditions display a centrally situated NF bundle that is prominently labeled with GFP along its length ('Filamentous'), some axonal neurites displayed only diffuse fluorescence within neurites ('Diffuse'), or smaller filamentous and punctate structures in addition to the filamentous bundle ('Mixed'). (B) Representative fluorescence images of cells treated with sense- or antisense-oriented MAP kinase oligonucleotides as indicated. Note the association of GFP with the NF bundle along the entire axonal length in cells receiving sense oligonucleotides, yielding a filamentous image and its absence in the distal neurite region in the presence of antisense oligonucleotides, yielding a diffuse pattern. (C) Percentage (mean±s.e.m.) of cells in which GFP-M was associated with the NF bundle in the distal third of the axonal length (as described in Materials and Methods) following treatment under various conditions as indicated in Fig. 2 and with SB202190, a p38 MAP kinase inhibitor. Note that PD98059, but not its carrier (DMSO) alone, antisense but not sense oligonucleotides and dominant-negative MAP kinase had reduced levels compared to the control. Note also that PD98059 did not prevent the increase induced by constitutively active MAP kinase.

NF bundle. We observed that alteration of MAP kinase activity had the identical impact on distribution of total axonal GFP-M as it did on association of GFP-M within the bundle: a 2-hour treatment with PD98059 reduced the ratio of distal/central GFP-M by 29.7±5.9%, whereas co-transfection with constitutively active MAP kinase increased this ratio by 39.2±10.8%. These data suggest that MAP kinase influenced overall NF axonal transport rather than just the incorporation of subunits into the central bundle.

These phenomena are not likely to result from overall alterations in axonal transport as the levels and distribution along axonal neurites of mitotracker-labeled vesicular structures were unchanged compared to those observed in control cells following treatment with PD98059 or expression of either constitutively active or dominant-negative MAP kinase (Fig. 4). Similarly, PD98059 did not alter the distribution of newly transported (CFP-tagged) tau within axonal neurites; unlike GFP-M, identical levels of CFP-htau40 were detected in the distal-most region of axonal neurites with or without treatment with PD98059 (Fig. 5).

Alteration of MAP kinase activity under these conditions did not compromise overall axonal architecture. Immunofluorescence analyses indicated that PD98059 treatment altered neither steady-state levels of tau, nor levels of tau phosphorylated at the PHF-1 or Tau-1 epitopes, within the distal portion of axonal neurites (Fig. 5). In addition, no change was observed in steady state levels of filamentous actin or MTs within axonal neurites following incubation with PD98059 (Fig. 6). Axonal neurite length was not altered by PD98059 or by expression of either constitutively active or dominant-negative MAP kinase (Fig. 6). This indicates that changes in distribution of GFP-M within this relatively short incubation period were not derived from retraction or extension of neurites, or from overall disruption in steady state levels of cytoskeletal proteins. Consistent with immunoblot analyses however, NF phospho-epitopes were reduced within neurites and perikarya (Fig. 6).

To examine more closely the mechanism(s) by which inhibition of MAP kinase prevented accumulation of filamentous GFP-M within distal region of axonal neurites, we captured sequential images of neurites prior to and following treatment with PD98059 and monitored translocation of GFP-labeled structures over time. As described previously for these cells (Yabe et al., 2001b) and for cultured sympathetic neurons

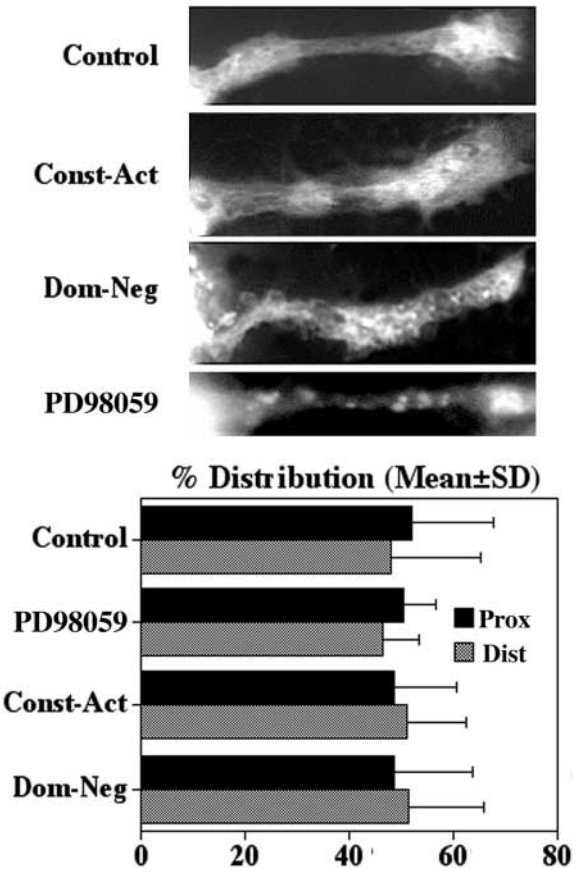

Fig. 4. MAP kinase does not alter the distribution of mitochondria within axonal neuritis. Representative mitotracker-labelled images of NB2a/d1 cells treated for 2 hours with the MAP kinase inhibitor PD98059 or transfected 24 hours previously with constructs of constitutively active (Const-Act) or dominant-negative (Dom-Neg) MAP kinase are shown along with untreated controls. The accompanying graph presents densitometric analyses of the fluorescent intensity of mitotracker within the distal (Dist) compared to the proximal (Prox) half of axonal neurites, expressed as the percentage (mean±s.d.) within the distal neurite. Note that the distribution of mitotracker-labeled structures was not altered by the above treatments.

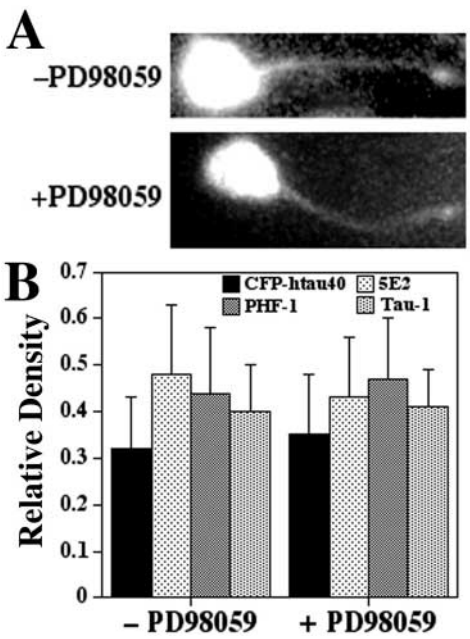

Fig. 5. Manipulation of MAP kinase activity does not alter the transport or distribution of tau within axonal neuritis. (A) Representative fluorescent images of NB2a/d1 cells transfected 24 hours previously with a construct expressing CFP-htau40 with (+) and without (–) treatment with the MAP kinase inhibitor PD98059 for 2 hours. (B) Graph of the relative density of CFP-htau40 fluorescence, along with PHF-1, Tau-1 and 5E2 immunoreactivity within axonal neurites determined from 50-100 cells in duplicate cultures with or without PD98059 treatment for 2 hours. Note that PD98059 did not alter the distribution of newly transported (CFP-tagged) tau within axonal neurites, nor that of phospho-dependent (PHF-1, Tau-1) or independent (5E2) tau epitopes.

(e.g. Wang and Brown, 2001), the majority of GFP-labeled structures, which consist of both filamentous and punctate forms, normally underwent transport in an anterograde direction. We examined the behavior of these smaller NFs and punctate structures following up- and down-regulation of MAP kinase activity. Considerable heterogeneity in the number of these structures was observed among axonal neurites (e.g. Fig. 7) (see also Yabe et al., 2001a; Yabe et al., 2001b); nevertheless, alteration of MAP kinase activity affected axonal transport regardless of the number of structures or predominant form of GFP-M. Quantification of GFP-tagged small NFs and punctate structures in multiple axonal neurites revealed that 66±9% (mean±s.e.m.) underwent anterograde transport. Of the remaining GFP-labeled structures, 15±4% underwent retrograde transport, and 19±2% exhibited no apparent motion during our limited observation period. Within 15 minutes of PD98059 treatment however, only 5±2% of GFP-tagged structures underwent anterograde transport, indicating a reduction of approximately 90%. The percentage of subunits undergoing retrograde transport was not as severely affected and was reduced to 11±5% (a reduction of approximately 26%). The percentage of subunits displaying no net motion increased to 84±6% in accord with the reduction in moving particles (Fig. 7). Treatment with DMSO (the carrier for PD98059) at an identical concentration as utilized in PD98059 treatment did not alter transport of GFP-containing structures (Fig. 7). Transport of mitotracker-labeled structures was not altered by treatment with PD98059 under these conditions (Fig. 7), confirming that PD98059 did not exert overall toxicity. SB202190, which inhibits the activity of p38 MAP kinase, did not alter transport of GFP-labeled structures (Figs 7, 8). The kinase inhibitor olomoucine, statistically inhibited transport of both GFP- and mitotracker-labeled elements (Figs 7, 8), consistent with reports that olomoucine inhibits all anterograde fast axonal transport (Ratner et al., 1998).

Continued treatment (e.g. 2-4 hours) with PD8059 shifted the balance of transport of GFP-tagged structures to retrograde, such that approximately 65% of small filamentous and punctate structures exhibited retrograde transport (Fig. 9). Protracted treatment with PD90859 eventually completely depleted small filamentous and punctate structures from axonal neurites and induced overall retraction of the GFP-labeled filamentous bundle, resulting in a reduction of total axonal GFP fluorescence of approximately 45% within 6 hours (Fig. 9). This effect was not a reflection of an overall shift of total axonal transport to retrograde, as the total fluorescent signal within axonal neurites derived from mitotracker-labeled vesicular structures was reduced only by approximately 10% over this same interval (Fig. 9). This modest reduction in mitotracker represents an identical level of reduction in fluorescent bleaching resulting from repeated imaging of the same axonal neurite without treatment with PD98059: a 15.8±0.9% reduction in GFP fluorescence and a 9.6±4% reduction in mitotracker fluorescence were observed following sequential capturing of images of otherwise untreated cells intensity for second versus first image (n=3 untreated neurites). In some instances, long-term treatment with PD98059 induced retraction of both ends, or apparent 'bunching' of NF bundles (i.e. retrograde retraction of the distal end along with anterograde coiling of both ends towards each other within the axonal hillock; Fig. 9).

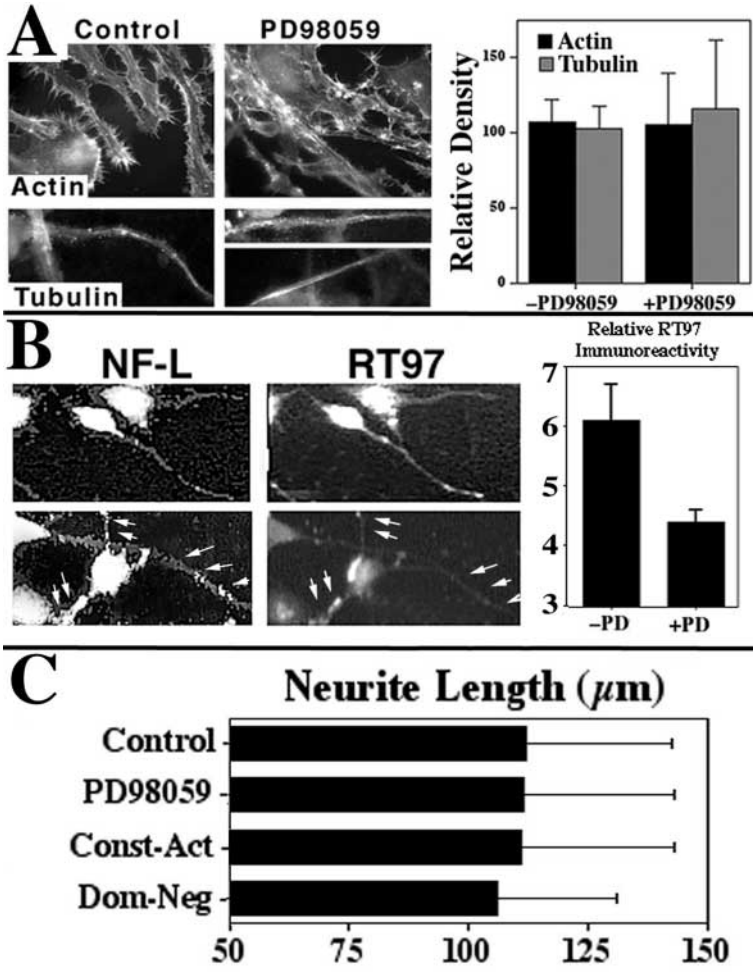

Fig. 6. Manipulation of MAP kinase activity does not alter neurite length or alter steady state levels of actin and tubulin, but does alter C-terminal NF phosphorylation within axonal neuritis. (A) Fluorescent images of axonal neurites of NB2a/d1 cells following labeling with rhodamine-conjugated phalloidin to label actin (Actin) or an anti-tubulin antibody (Tubulin). The accompanying graph shows the relative density of actin and tubulin fluorescence along axonal neurites ±2 hours' treatment with PD98059 determined for 25-50 cells (mean±s.d.); note that there is no significant difference in the presence or absence of PD98059. (B) Cells double-labeled with an antibody against NF-L and the phospho-dependent anti-NF antibody RT97. The graph shows the ratio of RT97 density/NF-L density (as indices of phospho-NFs and total NFs, respectively) before and after a 2-hour treatment with PD98059 (mean±s.d.). Treatment with PD98059 induced a specific reduction in phospho-NFs. (C) The length (mean±s.d.) of 25-50 axonal neurites in duplicate cultures following treatment with PD98059 or transfection with constitutively active (Const-Act) or dominant-negative (Dom-neg) MAP kinase. Axonal neurite length was not altered by manipulation of MAP kinase activity.

The above data demonstrate that alteration in MAP kinase activity alters both NF C-terminal phosphorylation and NF axonal transport. However, it remained possible that these

phenomena result from independent actions of MAP kinase. Alteration of NF axonal transport rate as a function of MAP kinase activity may actually be derived from changes in MAP kinase-mediated phosphorylation of NF motor proteins or linkers that maintain the association of NFs with their motor(s), rather than alteration in NF C-terminal phosphorylation. To address whether alteration in MAP kinase-mediated NF C-terminal phosphorylation directly impacted NF axonal transport, we transfected cells with constructs expressing wild-type (GFP-Hwt) NF-H conjugated to GFP, and the identical constructs in which serines in selected KSP domains known to be cdk5 phosphorylation sites have been mutated to aspartates (GFP-Hasp) to mimic a permanently phosphorylated state (Ackerley et al., 2003) (Fig. 10A). Consistent with the prior demonstration that cdk5 inhibits NF anterograde transport (Shea et al., 2004), this constitutively phosphorylated GFP-Hasp construct undergoes a slower transport rate than GFP-Hwt (Ackerley et al., 2003). It is unclear whether any or all of these mutated sites may be phosphorylated by MAP kinase. However, we reasoned that should MAP kinase promote

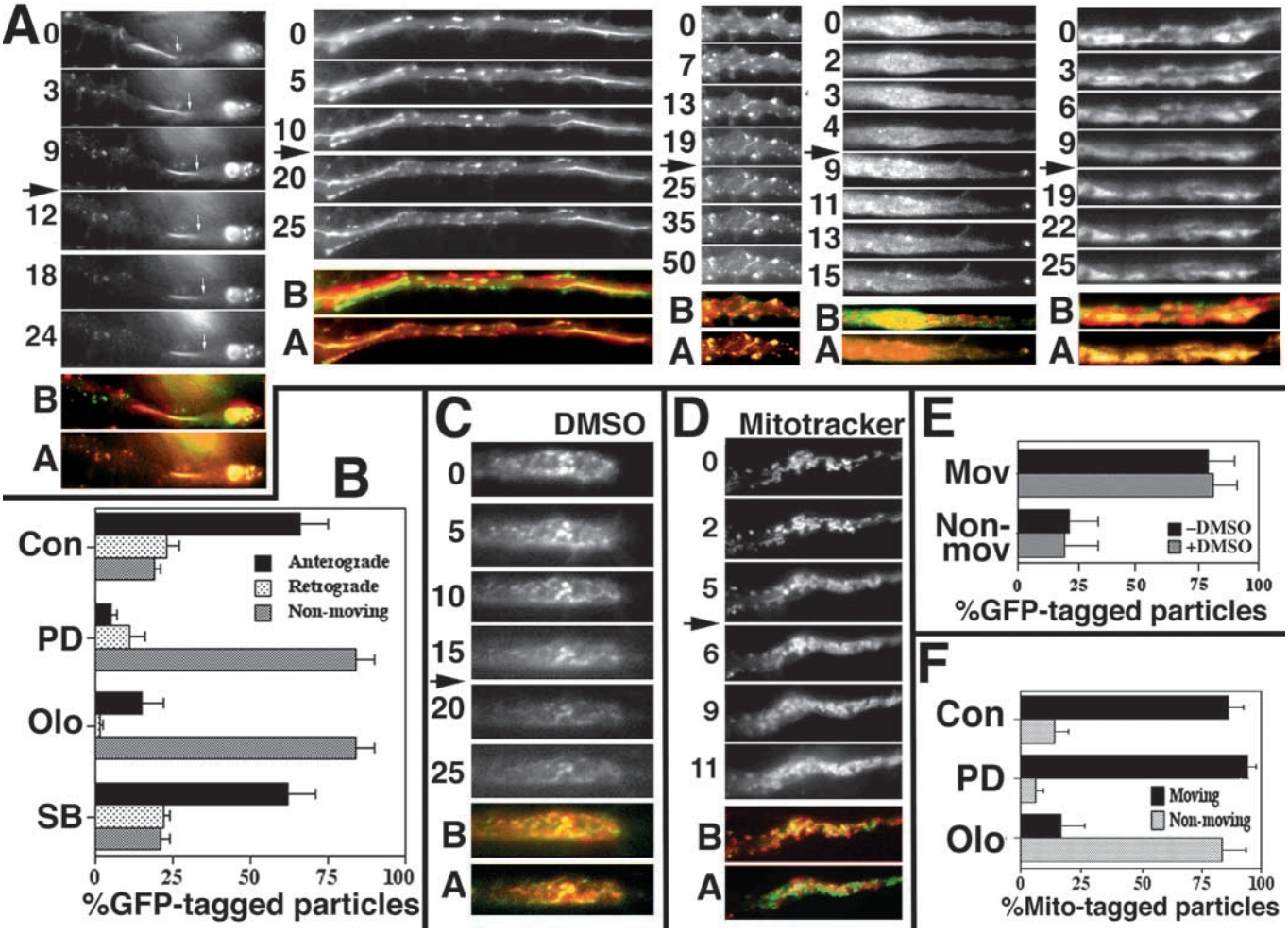

Fig. 7. Inhibition of MAP kinase activity inhibits NF axonal transport. (A,C,D) Sequentially captured images of axonal neurites of GFP-transfected NB2a/d1 cells (A,C) or mitotracker-stained cells (D) captured at the indicated intervals (in minutes) before and after addition of the MAP kinase inhibitor PD98059 (time of addition indicated by arrow). For each axonal neurite, one of the panels captured before PD98059 addition was false-colored green and a subsequent image was false-colored red and these images were then merged (indicated by B for before); the same procedure was carried out for two images captured after addition of PD98059 (indicated by A for after). Superimposing structures appear in yellow/orange, whereas non-superimposing structures remain red or green. This provides an additional index of the relative amount of moving versus stationary structures. Note that the majority of GFP-tagged structures do not superimpose prior to addition of PD98059, but do so following its addition (A), that PD98059 did not induce a similar increase in superimposing mitotracker-labeled structures (C) and that DMSO (carrier for PD98059) did not increase the number of superimposing GFP-tagged structures. Comparisons of images in overall sequences also indicate that PD98059 stopped the movement of GFP-tagged filamentous and particulate structures (A), did not affect the movement of mitotracker-labeled structures (C), and that DMSO did not affect the movement of GFP-tagged structures (D). (B) Percentage of filamentous or particulate GFP-tagged structures exhibiting net anterograde, retrograde or lack of net movement prior to (con, control) and following a 15-minute treatment with PD98059 (PD), olomoucine (Olo) or SB202190 (SB) as indicated. Note that PD98059 and olomoucine but not SB202190 dramatically increased the percentage of non-moving GFP-tagged structures. (E, F) Percentage of GFP-tagged (E) or mitotracker-labeled (F) particles exhibiting net motion in either the anterograde or retrograde direction (mov, 'moving') or no net motion (non mov, 'non moving') compiled from 5-10 individual axons. Note that the carrier DMSO (Con) and PD98059 itself did not alter the translocation of mitotracker-labeled particles, whereas olomoucine stopped translocation of approximately 80% of mitotracker-labeled particles.

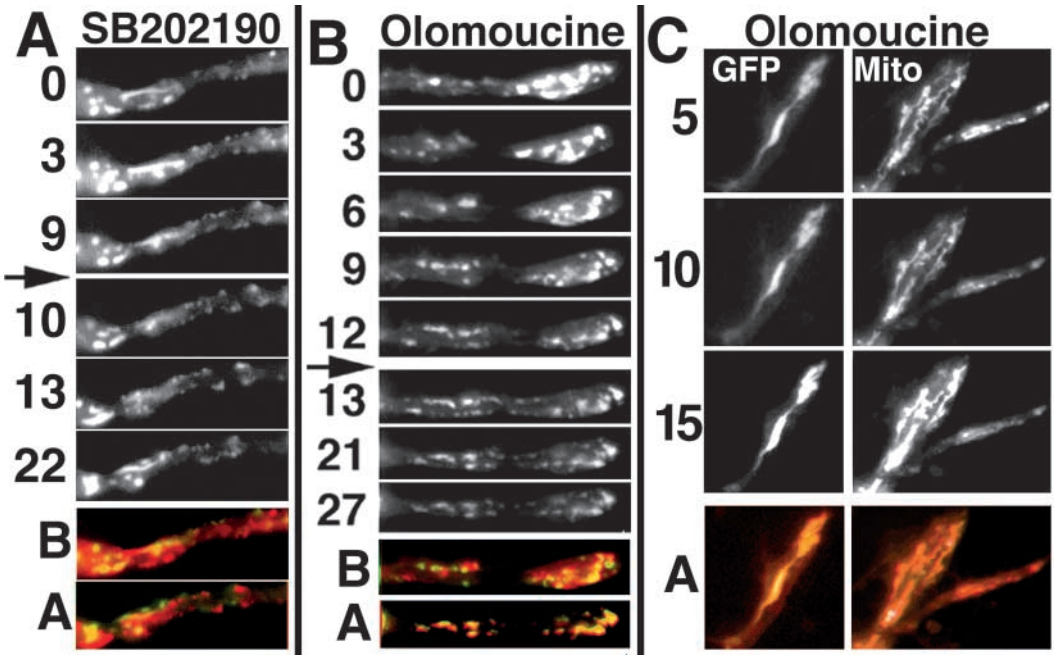

Fig. 8. SB202190 and olomoucine exert differential effects on NF transport in NB2a/d1 cells. (A-C) Sequential images of axonal neurites of GFP-M-transfected cells captured at the indicated intervals (in minutes) before and after addition of SB202190 (A) or olomoucine (B,C). The time of addition is indicated by the arrow in each case. (C) Images of cells 5-15 minutes after addition of olomoucine and mitotracker. Axonal neurites were imaged under fluorescent optics to visualize GFP and rhodamine optics to visualize mitotracker (Mito). False-color and merged images were prepared as described in the legend for Fig. 7 and in Materials and Methods. Note that SB202190 did not impair the transport of GFP-tagged structures (A). Note also that olomoucine inhibited transport of GFP-tagged structures, but did not inhibit transport of mitotracker-labeled structures in the same neurites (B,C).

anterograde NF transport by C-terminal sidearm phosphorylation of one or more of these mutated sites, anterograde transport of the GFP-Hasp construct may not be further inhibited by treatment with PD98059. Conversely, if the major impact of MAP kinase on NF transport is caused by something other than alterations in NF C-terminal phosphorylation, we anticipated that axonal transport of the GFP-Hasp and wild-type constructs would be similarly affected by PD98059. We monitored transport of these constructs as above both by quantifying the total level of GFP in the distal versus the central third of axonal neurites, as well as by real-time monitoring of the movement of GFP-tagged structures, before and after treatment with PD98059. A reduced distal/central ratio of total GFP was observed in GFP-HAsp-transfected versus GFP-Hwt-transfected cells. The day after transfection (when fluorescence is first consistently detectable within transfected cultures; see Materials and Methods), fluorescence intensity within the distal third of axonal neurites in cultures transfected with GFP-Hasp was only 64.2±0.9% of that in cultures transfected with GFP-Hwt. This correlates well with published results that GFP-Hasp undergoes transport at a rate approximately 65% of that of GFP-Hwt (Ackerley et al., 2003). Real-time monitoring of particle movement also yielded results similar to those reported previously (Ackerley et al., 2003): GFP-tagged structures in both GFP-Hwt- and GFP-Hasp-transfected cells displayed predominantly anterograde motion, with a minority of structures displaying retrograde motion and others pausing (defined as exhibiting no net motion over the observation period; Fig. 10D,E). We therefore conclude that GFP-H-asp and GFP-Hwt display similar transport kinetics in differentiated NB2a/d1 cells as previously demonstrated for cultured cortical neurons (Ackerley et al., 2003). We next compared the effect of inhibition of MAP kinase upon the transport of these constructs. The percentages of GFP-tagged particles in both GFP-Hwt- and GFP-HAsp-transfected NB2a/d1 cells undergoing anterograde or retrograde transport or not exhibiting any transport during the observation period (Fig. 10E) were similar to those observed for GFP-M (Fig. 7). The response of cells transfected with GFP-Hwt to PD98059 was also similar to that of cells transfected with GFP-M. However, cells transfected with GFP-Hasp were markedly less responsive to PD98059. As with GFP-M, the majority (71±10%) of anterogradely transporting GFP-tagged structures in GFP-Hwt-transfected cells ceased net translocation within 15 minutes of application of PD98059. By contrast, only ~33±9% of anterogradely transporting GFP-tagged structures ceased net translocation in GFP-Hasp-transfected cells during this time, resulting in twice as many anterogradely transporting GFP-tagged structures maintaining anterograde transport following a 15-minute treatment with PD98059 in cells transfected with GFP-H-asp compared to those transfected with GFP-Hwt ($P<0.05$; Student's *t*-test; Fig. 10E). Failure of the constitutively phosphorylated construct to cease anterograde transport following treatment with PD98059 is consistent with the notion that MAP kinase-mediated phosphorylation of key sites within the C-terminal region of NF-H supports NF anterograde axonal transport. These constructs also yielded differing responses to longer (2-hour) treatment with PD98059, which increased retrograde transport of GFP-M (Fig. 9). GFP-Hwt fluorescence within distal axonal

regions was reduced by 34.8±5.2% following 2-hour treatment with PD98059 (P<0.04, before versus after PD98059 treatment; Student's t-test). By contrast, GFP-Hasp fluorescence was not significantly reduced (12.4±14.7%; P<0.26, before versus after PD98059 treatment; Student's t-test; Fig. 10C). These data indicate that NF-H sidearm phosphorylation interferes with the increase in retrograde transport normally observed following long-term treatment with PD98059 (Fig. 9) and therefore support the conclusion that MAP kinase promotes anterograde NF axonal transport and/or inhibits retrograde NF transport and at least in part, phosphorylation of the C-terminus of NF-H.

Discussion

We demonstrate that p42/44 MAP kinase promotes NF axonal transport and consistent with prior studies (Li et al., 1999; Veeranna et al., 1998), phosphorylates the C-terminus of NF-H and NF-M. Increased C-terminal NF phosphorylation has generally been considered to interfere with axonal transport, as accumulation of phospho-NFs within perikarya or proximal neurons accompanies certain neurodegenerative conditions (for reviews, see Grant and Pant, 2000; Julien, 1999). Similarly, hyperactivation of NF C-terminal kinases has been considered as one likely mechanism leading to disruption in normal NF distribution (Grant and Pant, 2000; Julien, 1999; Miller et al., 2002). Overexpression of the NF C-terminal kinase cdk5 (Shea et al., 2004), and treatment with glutamate (which activated SAP and MAP kinases) (Ackerley et al., 2000), each increased NF C-terminal phosphorylation and induced the accumulation of phospho-NFs within perikarya. We therefore anticipated that directly increasing MAP kinase activity would also impair NF axonal transport, especially as disregulation/over-amplification of the p42/44 MAP kinase can lead to neurodegeneration (e.g. Ekinci et al., 1999; Koistinaho and Koistinaho, 2002; Schroeter et al., 2002). However, despite increasing C-terminal NF phosphorylation within intact neuronal cells, we observed that MAP kinase promotes, rather than inhibits, NF transport. These data suggest that cdk5 and MAP kinase exert opposing influences on NF anterograde axonal transport, and confirm that the relationship of C-terminal NF phosphorylation to NF axonal transport and interaction is complex.

Hypophosphorylated NF subunits co-precipitate with kinesin and addition of MAP kinase to such preparations phosphorylates NF subunits and disrupts co-precipitation (Yabe et al., 2000). As the anterograde motor protein kinesin participates in transport of NF subunits into axonal neurites (Yabe et al., 1999), dissociation of NFs from an anterograde motor by MAP kinase under cell-free conditions seems at odds with the observed promotion of NF anterograde transport by MAP kinase within intact cells. One possible explanation is that MAP kinase-mediated dissociation of NF subunits from kinesin under cell-free conditions resulted from non-physiological hyperphosphorylation of NF subunits and/or kinesin linker protein(s). Alternatively, C-terminal NF

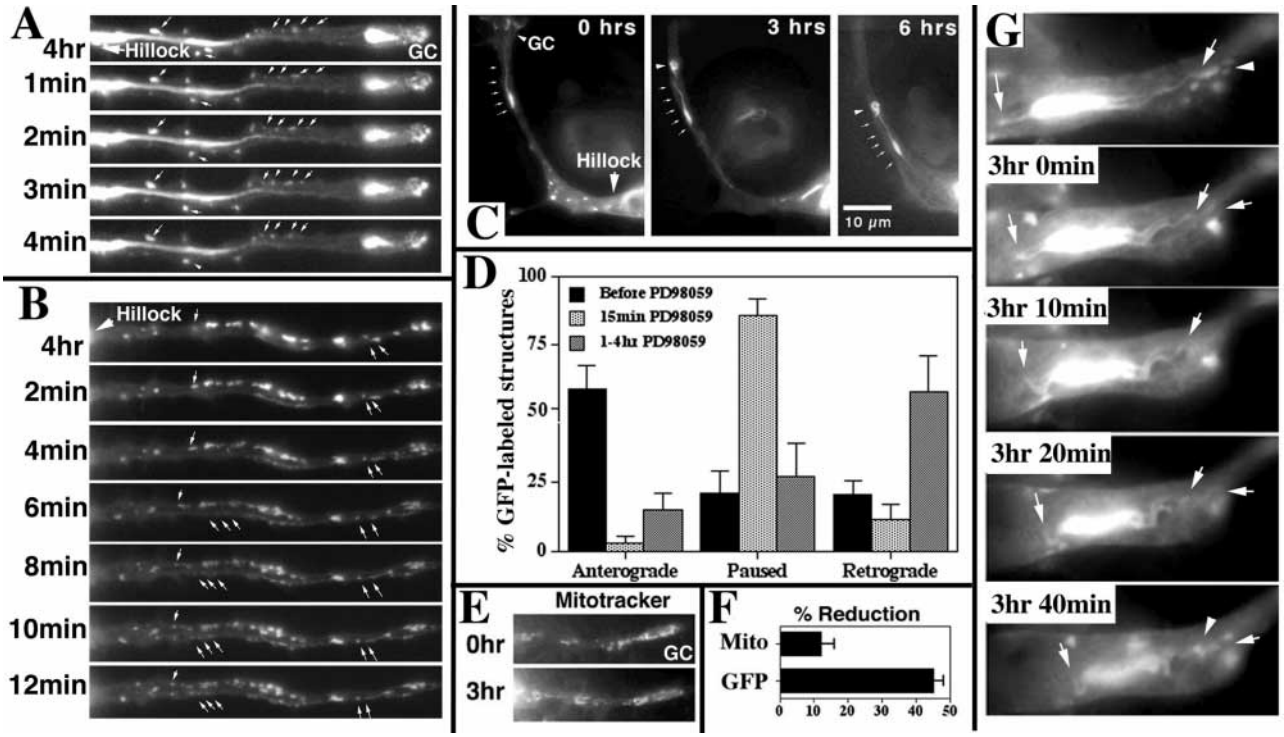

Fig. 9. Long-term inhibition of MAP kinase activity induces net retrograde NF transport. (A-C,E,G) GFP-transfected (A-C,G) and mitotracker-labeled (E) NB2a/d1 cells sequentially captured at the indicated intervals following treatment with PD98059. Selected GFP-tagged structures undergoing retrograde transport are indicated by arrows; not all such structures are indicated. (D) Data derived from over 100 individual GFP-tagged structures from multiple cultures from three experiments. Note that this more prolonged treatment with PD98059 induces a shift from net anterograde to net retrograde transport of GFP-tagged structures. Note that treatment with PD98059 for 3 hours did not reduce the overall level of mitotracker-labeled structures within axonal neurites (E, F). GC in panel C denotes the growth cone (Hillock). Scale bar in C (refers to all panels), 10 μm.

phosphorylation derived from p42/44 MAP kinase may be essential to promote NF-NF associations leading to 'bundling' within axons (Yabe et al., 2001a). MAP kinase may foster dissociation of NF subunits from their anterograde motor, perhaps via the same or additional phosphorylation events, and promote phospho-dependent NF bundling (Yabe et al., 2001a; Shea and Yabe, 2000). Compromise in the development of sufficient phospho-dependent NF-NF associations, coupled with dissociation of NFs from their anterograde transport system, might foster the observed net shift to retrograde transport. Notably, multiple NF kinases have been reported with distinct target sites; alterations in regulation of p42/44 MAP kinase may impair sequential phosphorylation by a distinct NF kinase, or place subunits at risk for inappropriate phosphorylation by a distinct kinase, leading to perturbations in NF transport and distribution. As the reduced impact of PD98059 on a constitutively phosphorylated NF-H construct (GFP-Hasp) supports the conclusion that p42/44 MAP kinase promotes anterograde NF transport by phosphorylation of NF-H sidearm phosphorylation, it also remains possible that cessation of anterograde NF transport following inhibition of p42/44 MAP kinase is due at least in part to decreased phosphorylation of other constituents, such as anterograde motors and/or linker proteins. In this regard, a second NF kinase, GSK-3B regulates the association of vesicular cargo with kinesin (Paglini et al., 2001); the influence of this kinase on transport of NFs has not been determined as yet. In addition, p42/44 MAP kinase has been proposed to regulate transport of vesicular elements, perhaps by associating with molecular motors (Kholodenko, 2002). Any putative influence of MAP kinase on motors and/or linkers would have to be confined to a subset, rather than all, linkers, as anterograde transport of

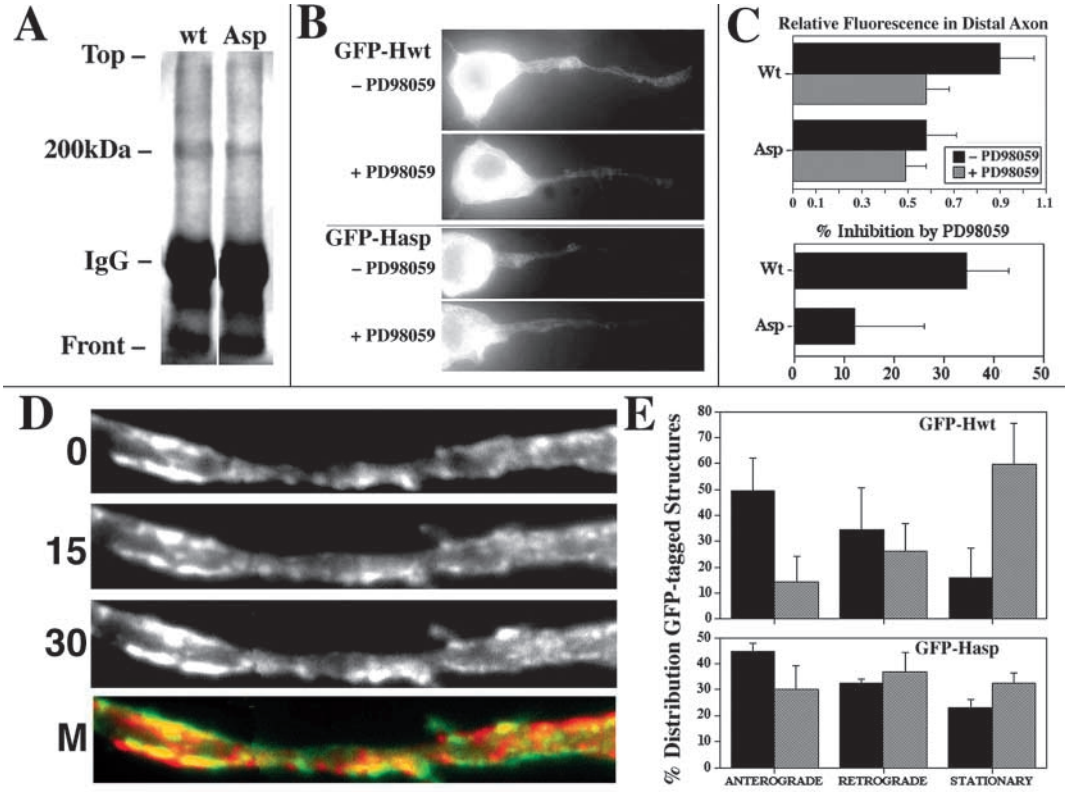

Fig. 10. Inhibition of MAP kinase affects the distribution of normal and constitutively phosphorylated NF-H within axonal neurites equally. (A) Immunoprecipitation with anti-NF polyclonal antibody R39 from cultures transfected 24 hours previously with GFP-Hwt (wt) or GFP-Hasp (Asp) and probed with anti-GFP antibody; note the presence of GFP-immunoreactive species migrating at ~200 kDa. (B) Representative images of cells transfected with GFP-Hwt or GFP-Hasp as indicated, before and after 2 hours' treatment with PD98059; images before and after treatment are of different cells. (C) Densitometric analysis of the ratio of GFP fluorescence in the distal versus the central third of axonal neurites from 10-20 individual cells from two independent experiments before and after a 2-hour treatment with PD98059. The lower graph shows the percentage reduction in GFP signal in the distal third of axonal neurites for each construct following a 2-hour treatment with PD98059, obtained by dividing the ratio before to that after treatment. Consistent with prior reports (see text), the ratio of GFP signal in distal/central axons is lower in cells transfected with GFP-Hasp compared to GFP-Hwt; however, note that 2 hours' treatment with PD98059 reduces this ratio by the same percentage for both constructs. A similar impression is obtained by visual inspection of the cells in panel B. (D) Sequentially captured images of representative axonal neurites of a cell transfected with GFP-Hasp at 15-second intervals commencing 15 minutes after addition of PD98059. The merged image (M) was prepared from the 0 and 30 second images as described in the legend for Fig. 7. Note that many structures in the merged image do not superimpose indicating continued net translocation following the addition of PD98059. (E) The percentage of filamentous or particulate GFP-tagged structures exhibiting net anterograde, retrograde or lack of net movement prior to (dark-shaded bars) and following (pale-shaded bars) a 15-minute treatment with PD98059 from 10-20 individual axons from two independent experiments for each construct quantified as described in Materials and Methods and in the legend to Fig. 7. Images of cells transfected with GFP-Hwt and of cells transfected with GFP-Hasp prior to the addition of PD98059 are not presented because, as indicated by quantification of particles (E) they are essentially identical to those presented for GFP-M in Fig. 7.

mitotracker-labeled vesicular structures, as well as that of another axonal cytoskeletal protein, tau, was not altered following manipulation of MAP kinase activity.

The role of NF C-terminal phosphorylation in axonal transport has recently been questioned (Rao et al., 2003; Shea et al., 2003). However, our findings support the notion that NF-H C-terminal phosphorylation plays a role in NF axonal transport, as, consistent with the findings of Ackerley et al. (Ackerley et al., 2003), the relative level of GFP-Hasp within the distal third of neurites was reduced compared to that of GFP-Hwt. Despite this phosphorylation-mediated reduction in anterograde transport, this constitutively phosphorylated construct was less sensitive to inhibition of MAP kinase, supporting the interpretation that MAP kinase-mediated phosphorylation of NFs promotes their anterograde transport. These data support the possibility that phosphorylation at distinct sites, perhaps mediated by multiple kinases, may have additive and/or opposing effects on NF transport (see also Zhang et al., 2003). Although the data are consistent with the interpretation that MAP kinase promotes anterograde NF transport at least in part by C-terminal NF phosphorylation, this does not eliminate the possibility that MAP kinase also influences NF transport by phosphorylation of one or more motors and/or linker proteins. An additional possibility is that MAP kinase promotes anterograde NF transport somewhat indirectly by preventing the association of NFs with a competing retrograde motor; this could also be accomplished by either NF C-terminal phosphorylation and/or phosphorylation of retrograde motor(s) and/or their linkers (Shea and Flanagan, 2001).

The impact of alterations in activity of multiple kinases may be useful to discern the full relationship between C-terminal phosphorylation and NF transport. In this regard, p42/44 MAP kinase and p38 MAP kinase apparently exert differential effects on NF transport, as PD98059 (which inhibits p42/44 activity) inhibited transport of NFs whereas SB202190 (which inhibits p38 activity) did not. Increased or decreased p42/44 activity did not alter mitochondrial transport in our experiments, whereas p38 activity inhibits mitochondrial transport (De Vos et al., 2000), suggesting that these two members of the MAP kinase family may exert differential effects on transport of other elements as well. As inhibition of p38 activity increases p42/44 activity (Singh et al., 1999), it would be interesting to monitor the combined influence of alterations in these two kinases on NF distribution and/or overall axonal transport. Similarly, cdk5, which regulates fast anterograde transport of NFs (Shea et al., 2004) and vesicular cargo (Paglini et al., 2001; Ratner et al., 1998), inhibits p42/44 MAP activity (Sharma et al., 2002). Our findings leave open the possibility that cdk5, which promotes the accumulation of phospho-NFs within neuronal perikarya (Bajaj et al., 1998), does so in part by inhibiting MAP kinase, thereby indirectly inhibiting anterograde transport and increasing perikaryal NFs. This possibility is supported by the demonstration that both cdk5 and P42/44 MAP kinase are associated with cytoskeletal complexes that contain NF subunits in brain (Veeranna et al., 2000). Notably, olomoucine as utilized in the present study inhibited axonal transport of NFs, which is consistent with the prior report that olomoucine inhibited overall axonal transport (Ratner et al., 1998). Although olomoucine is active against cdk5, transfection-mediated increase in cdk5 activity diminished NF axonal transport, whereas another inhibitor active against cdk5 (roscovitine) promoted it. These data collectively suggest that olomoucine may exert its effect on NF axonal transport by inhibiting one or more kinases instead of or in addition to cdk5.

In prior studies demonstrating that glutamate impairs NF anterograde axonal transport, both p42/44 MAP kinase and SAP kinases were activated, leading the authors to suggest that either or both of these NF kinases may be responsible for glutamate-induced inhibition of anterograde NF transport (Ackerley et al., 2000; Brownlees et al., 2000). Our data support the possibility that increased SAP kinase activity, rather than increased activity of p42/44 MAP kinase, mediated the glutamate-induced inhibition of NF axonal transport. Although activation of either SAP (Brownlees et al., 2000; Giasson and Mushynski, 1996; O'Ferrall et al., 2000) or p42/44 MAP kinase (shown herein) increases NF phosphorylation our data demonstrates that activation of p42/44 MAP kinase increases rather than inhibits, NF anterograde axonal transport. Of interest therefore, would be to determine the influence of direct inhibition of SAP kinase on NF axonal transport. It should also be considered that the impact of alterations in kinase activities may not necessarily reflect normal kinase function, but may instead at least in part represent artifacts resulting from kinase overexpression or inappropriate levels of inhibition.

Our findings indicate that MAP kinase does not regulate axonal transport of tau at least to the degree to which it regulates transport of NFs. We did not carry out an exhaustive examination of tau, actin or MT dynamics and our limited data in this area should not be interpreted as indicating that MAP kinase does not regulate the dynamics of one or more of these proteins at some level. However, overexpression of tau in these cells affects bidirectional transport of other vesicles and organelles, apparently by interfering with their association with transport machinery. Tau overexpression eventually shifts the balance of NF transport in favor of net retrograde transport, and fosters the accumulation of NF clusters within perikarya (Stamer et al., 2002; Trinczek et al., 1999). As MAP kinase phosphorylates tau (Drewes et al., 1992; Lu et al., 1993; Roeder et al., 1993; Shea, 1997), there may be some as yet undisclosed interaction between tau and NFs that is modulated by MAP kinase.

Promotion of NF transport by p42/44 MAP kinase is consistent with the pivotal role of this kinase in development of the nervous system. The MAP kinase pathway mediates both neurogenesis and neuronal differentiation; stimulation of the MAP kinase pathway by epidermal growth factor induces neuronal proliferation, whereas stimulation by nerve growth factor induces differentiation (Vaudry et al., 2002). MAP kinase activity is furthermore required for multiple aspects of neuronal remodeling, including neurite outgrowth (Obara et al., 2002; Tang, 2003), axonal branching (Abe et al., 2001), dendrite formation (Valliant et al., 2002) and synaptic plasticity (Koh et al., 2002), as well as various non-neuronal cellular remodeling processes including oocyte and spermatocyte maturation (Kotani and Yamashita, 2002; Sette et al., 1999; Sun et al., 2002), spindle formation, chromatin condensation and nuclear reorganization following division (Lu et al., 2002; Stone et al., 2000) and cell migration (Nakamura et al., 2001). The data of the present study suggest that MAP kinase also participates in

the stabilization of developing axons by promoting the accumulation of NFs within growing axonal neurites.

This research was supported by the National Science Foundation. We thank Dr Ron Liem for his NF-M cDNA, Dr E. Mandelkow for the tau construct and Dr C. Miller for his neurofilament constructs.

References

Abe, K., Aoyagi, A. and Saito, H. (2001). Sustained phosphorylation of mitogen-activated protein kinase is required for basic fibroblast growth factor-mediated axonal branch formation in cultured rat hippocampal neurons. *Neurochem. Int.* **38**, 309-315.

Ackerley, S., Grierson, A. J., Brownlees, J., Thornhill, P., Anderton, B. H., Leigh, P. N., Shaw, C. E. and Miller, C. C. (2000). Glutamate slows axonal transport of neurofilaments in transfected neurons. *J. Cell Biol.* **150**, 165-176.

Ackerley, S., Thornhill, P., Grierson, A. J., Brownlees, J., Anderton, B. H., Leigh, P. N., Shaw, C. E. and Miller, C. (2003). Neurofilament heavy chain side-arm phosphorylation regulates axonal transport of neurofilaments. *J. Cell Biol*, **161**, 489-495.

Alessi, D. R., Cuenda, A., Cohen, P., Dudley, D. T. and Saltiel, A. D. (1995). PD98059 is a specific inhibitor of the activation of mitogen-activated protein kinase in vitro and in vivo. *J. Biol. Chem.* **270**, 4220-4227.

Bajaj, N. P., Al-Sarraj, S. T., Anderson, V., Kibble, M., Leigh, N. and Miller, C. C. (1998). Cyclin-dependent kinase-5 is associated with lipofuscin in motor neurones in amyotrophic lateral sclerosis. *Neurosci. Lett.* **245**, 45-48.

Brownlees, J., Yates, A., Bajaj, N. P., Davis, D., Anderton, B. H., Leigh, P. N., Shaw, C. E. and Miller, C. C. (2000). Phosphorylation of neurofilament heavy chain side-arms by stress activated protein kinase-1b/Jun N-terminal kinase-3. *J. Cell Sci.* **113**, 401-407.

Cobb, M. H. (1999). MAP kinase pathways. *Prog. Biophys. Mol. Biol.* **71**, 479-500.

Cuenda, A., Rouse, J., Doza, Y. N., Meier, R., Cohen, P., Gallagher, T. F., Young, P. R. and Lee, J. C. (1995). SB203580 is a specific inhibitor of a MAP kinase homologue which is stimulated by cellular stresses and interleukin-1. *FEBS Lett.* **364**, 229-233.

De Vos, K., Severin, F., van Herreweghe, F., Vancompernolle, K., Goossens, V., Hyman, A. and Grooten, J. (2000). Tumor necrosis factor induces hyperphosphorylation of kinesin light chain and inhibits kinesin-mediated transport of mitochondria. *J. Cell Biol.* **149**, 1207-1214.

Drewes, G., Lichtenberg-Kraag, B., Doring, F., Mandelkow, E. M., Biernat, J., Goris, J., Doree, M. and Mandelkow, E. (1992). Mitogen activated protein (MAP) kinase transforms tau protein into an Alzheimer-like state. *EMBO J.* **11**, 2131-2138.

Ekinci, F. J., Malik, K. M. and Shea, T. B. (1999). beta-amyloid induces calcium influx and neurodegeneration by MAP kinase-mediated activation of the L voltage-sensitive calcium channel. *J. Biol. Chem.* **274**, 30322-30327.

Giasson, B. I. and Mushynski, W. E. (1996). Aberrant stress-induced phosphorylation of perikaryal neurofilaments. *J. Biol. Chem.* **271**, 30404-30409.

Giasson, B. I. and Mushynski, W. E. (1997). Study of proline-directed protein kinases involved in phosphorylation of the heavy neurofilament subunit. *J. Neurosci.* **17**, 9466-9472.

Grant, P. and Pant, H. C. (2000). Neurofilament protein synthesis and phosphorylation. *J. Neurocytol.* **29**, 843-872.

Greenberg, S. G. and Davies, P. (1990). A preparation of Alzheimer paired helical filaments that displays distinct tau proteins by polyacrylamide gel electrophoresis. *Proc. Natl. Acad. Sci. USA* **87**, 5827-5831.

Guidato, S., Tsai, L. H., Woodgett, J. and Miller, C. C. J. (1996). Differential cellular phosphorylation of neurofilament heavy side-arms by glycogen synthase kinase-3 and cyclin-dependent kinase-5. *J. Neurochem.* **66**, 1698-1706.

Gou, J. P., Gotow, T., Janmey, P. A. and Leterrier, J. F. (1998). Regulation of neurofilament interactions in vitro by natural and synthetic polypeptide sequences within the heavy neurofilament subunit NF-H: neurofilament crossbriding by antiparallel sidearm overlapping. *Med. Biol. Eng. Comp.* **36**, 371-387.

Hirokawa, N., Glicksman, M. A. and Willard, M. B. (1984). Organization of mammalian neurofilament polypeptides within the neuronal cytoskeleton. *J. Cell Biol.* **98**, 1523-1536.

Hoffman, P. N. and Lasek, R. J. (1975). The slow component of axonal transport. Identification of major structural polypeptides of the axon and their generality among mammalian neurons. *J. Cell Biol.* **66**, 351-366.

Hoffman, P. N., Griffin, J. W. and Price, D. L. (1984). Control of axonal caliber by neurofilament transport. *J. Cell Biol.* **99**, 705-714.

Johnson, G. L. and Lapadat, R. (2002). Mitogen-activated protein kinase pathways mediated by ERK, JNK, and p38 protein kinases. *Science* **298**, 1911-1912.

Joachim, C. L., Morris, J. H., Selkoe, D. J. and Kosik, K. S. (1987). Tau epitopes are incorporated into a range of lesions in Alzheimer's disease. *J. Neuropathol. Exp. Neurol.* **46**, 611-622.

Julien, J. P. (1999). Neurofilament functions in health and disease. *Curr. Opin. Neurobiol.* **9**, 554-560.

Julien, J. P. and Mushynski, W. E. (1983). The distribution of phosphorylation sites among identified proteolytic fragments of mammalian neurofilaments. *J. Biol. Chem.* **258**, 4019-4025.

Julien, J. P. and Mushynski, W. E. (1998). Neurofilaments in health and disease. *Prog. Nucleic Acids Res. Mol. Biol.* **61**, 1-20.

Jung, C. and Shea, T. B. (1999). Regulation of neurofilament axonal transport by phosphorylation in optic axons in situ. *Cell. Motil. Cytoskel.* **43**, 230-240.

Jung, C. and Shea, T. B. (2004). Neurofilament subunits undergo more rapid translocation within retinas than in optic axons. *Brain Res. Mol. Brain Res.* **122**, 188-192.

Jung, C., Yabe, J., Wang, F. S. and Shea, T. B. (1998). Neurofilaments are present within axonal neurites before incorporation into Triton-insoluble structures. *Cell. Motil. Cytoskel.* **40**, 44-58.

Jung, C., Yabe, J. T. and Shea, T. B. (2000a). C-terminal phosphorylation of the heavy molecular weight neurofilament subunit is inversely correlated with neurofilament axonal transport velocity. *Brain Res.* **856**, 12-19.

Jung, C., Yabe, J. T., Lee, S. and Shea, T. B. (2000b). Hypophosphorylated neurofilament subunits undergo axonal transport more rapidly than more extenisvely phosphorylated subunits in situ. *Cell. Motil. Cytoskel.* **47**, 120-129.

Kholodenko, B. N. (2002). MAP kinase cascade signaling and endocytic trafficking, a marriage of convenience? *Trends Cell Biol.* **12**, 173-177.

Koh, Y. H., Ruiz-Canada, C., Gorczyca, M. and Budnik, V. (2002). The Ras1-mitogen-activated protein kinase signal transduction pathway regulates synaptic plasticity through fasciclin II-mediated cell adhesion. *J. Neurosci.* **22**, 2496-2504.

Koistinaho, M. and Koistinaho, J. (2002). Role of p38 and p44/42 mitogen-activated protein kinases in microglia. *Glia* **40**, 175-183.

Kosik, K. S., Crandall, J. E., Mufson, E. J. and Neve, R. L. (1989). Tau in situ hybridization in normal and Alzheimer brain: localization in the somatodendritic compartment. *Ann. Neurol.* **26**, 352-361.

Kotani, T. and Yamashita, M. (2002). Discrimination of the roles of MPF and MAP kinase in morphological changes that occur during oocyte maturation. *Dev. Biol.* **252**, 271-286.

Leterrier, J. F., Käs, J., Hartwig, J., Vegners, R. and Janmey, P. (1996). Mechanical effects of neurofilament cross-bridges. *J. Biol. Chem.* **271**, 15687-15694.

Lewis, S. E. and Nixon, R. A. (1988). Multiple phosphorylated variants of the high molecular mass subunit of neurofilaments in axons of retinal cell neurons: characterization and evidence for their differential association with stationary and moving neurofilaments. *J. Cell Biol.* **107**, 2689-2701.

Li, B. S., Veeranna Gu, J., Grant, P. and Pant, H. C. (1999). Activation of mitogen-activated protein kinases (Erk1 and Erk 2) cascade results in phosphorylation of NF-M tail domains in transfected NIH 3T3 cells. *Eur. J. Biochem.* **262**, 211-217.

Lu, Q., Soria, J. P. and Wood, J. G. (1993). p44mpk MAP kinase induces Alzheimer type alterations in tau function and in primary hippocampal neurons. *J. Neurosci. Res.* **35**, 439-444.

Lu, Q., Dunn, R. L., Angeles, R. and Smith, G. D. (2002). Regulation of spindle formation by active mitogen-activated protein kinase and protein phosphatase 2A during mouse oocyte meiosis. *Biol. Reprod.* **66**, 29-37.

Manthey, C. L., Wang, S. W., Kinney, S. D. and Yao, Z. (1998). SB202190, a selective inhibitor of p38 mitogen-activated protein kinase, is a powerful regulator of LPS-induced mRNAs in monocytes. *J. Leukoc. Biol.* **64**, 409-417.

Miller, C. C. J., Ackerley, S., Brownlees, J., Grierson, A. J., Jacobsen, N. J. O. and Thornhill, P. (2002). Axonal transport of neurofilaments in normal and disease states. *Cell. Mol. Life Sci.* **59**, 323-330.

Nakamura, T., Mochizuki, Y., Kanetake, H. and Kanda, S. (2001). Signals via FGF receptor 2 regulate migration of endothelial cells. *Biochem. Biophys. Res. Commun.* **289**, 801-806.

Nixon, R. A. and Shea, T. B. (1992). Dynamics of neuronal intermediate filaments: a developmental perspective. *Cell Motil. Cytoskel.* **22**, 81-91.

Nixon, R. A., Lewis, S. E. and Marotta, C. A. (1987). Posttranslational modification of neurofilament proteins by phosphate during axoplasmic transport in retinal ganglion cell neurons. *J. Neurosci.* **4**, 1145-1158.

Nixon, R. A., Paskevich, P. A., Sihag, R. K. and Thayer, C. Y. (1994). Phosphorylation on carboxyl terminus domains of neurofilament proteins in retinal ganglion cell neurons in vivo: influences on regional neurofilament accumulation, interfilament spacing and axonal caliber. *J. Cell Biol.* **126**, 1031-1046.

Obara, Y., Aoki, T., Kusano, M. and Ohizumi, Y. (2002). Beta-eudesmol induces neurite outgrowth in rat pheochromocytoma cells accompanied by an activation of mitogen-activated protein kinase. *J. Pharmacol. Exp. Ther.* **3**, 803-811.

O'Ferrall, E. K., Robertson, J. and Mushynski, W. E. (2000). Inhibition of aberrant and constitutive phosphorylation of the high-molecular-mass neurofilament subunit by CEP-1347 (KT7515), an inhibitor of the stress-activated protein kinase signaling pathway. *J. Neurochem.* **75**, 2358-2367.

Paglini, G., Peris, L., Diez-Guerra, J., Quiroga, S. and Caceres, A. (2001). The Cdk5-p35 kinase associates with the Golgi apparatus and regulates membrane traffic. *EMBO J.* **2**, 1139-1144.

Pang, L., Sawada, T., Decker, S. J. and Saltiel, A. R. (1995). Inhibition of MAP kinase blocks the differentiation of PC-12 cells induced by nerve growth factor. *J. Biol. Chem.* **270**, 13585-13588.

Pant, H. C. (1988). Dephosphorylation of neurofilament protein enhances their susceptibility to degradation by calpain. *Biochem. J.* **256**, 665-668.

Pant, H. C. and Veeranna (1995). Neurofilament phosphorylation. *Biochem. Cell Biol.* **73**, 575-592.

Rao, M. V., Garcia, M. L., Miyazaki, Y., Gotow, T., Yuan, A., Mattina, S., Ward, C. M., Calcutt, N. A., Uchiyama, Y., Nixon, R. A. et al. (2002). Gene replacement in mice reveals that the heavily phosphorylated tail of neurofilament heavy subunit does not affect axonal caliber or the transit of cargoes in slow axonal transport. *J. Cell Biol.* **158**, 681-693.

Ratner, N., Bloom, G. S. and Brady, S. T. (1998). A role for cyclin-dependent kinases(s) in the modulation of fast axonal transport: effects defined by olomoucine and the APC supressor protein. *J. Neurosci.* **18**, 7717-7726.

Roder, H. M., Eden, P. A. and Ingram, V. M. (1993). Brain protein kinase PK40erk converts TAU into a PHF-like form as found in Alzheimer's disease. *Biochem. Biophys. Res. Commun.* **193**, 639-647.

Sanchez, I., Hassinger, L., Sihag, R. K., Cleveland, D. W., Mohan, P. and Nixon, R. A. (2000). Local control of neurofilament accumulation during radial growth of myelinating axons in vivo: selective role of site-specific phosphorylation. *J. Cell Biol.* **151**, 1013-1024.

Schroeter, H., Boyd, C., Spencer, J. P., Williams, R. J., Cadenas, E. and Rice-Evans, C. (2002). MAPK signaling in neurodegeneration: influences of flavonoids and of nitric oxide. *Neurobiol. Aging* **23**, 861-880.

Sette, C., Barchi, M., Bianchini, A., Conti, M., Rossi, P. and Geremia, R. (1999). Activation of the mitogen-activated protein kinase ERK1 during meiotic progression of mouse pachytene spermatocytes. *J. Biol. Chem.* **274**, 33571-33579.

Sharma, M., Sharma, P. and Pant, H. C. (1999). CDK-5-mediated neurofilament phosphorylation in SHSY5Y human neuroblastoma cells. *J. Neurochem.* **73**, 79-86.

Sharma, P., Veeranna, Sharma, M., Amin, N. D., Sihag, R. K., Grant, P., Ahn, N., Kulkarni, A. B. and Pant, H. C. (2002). Phosphorylation of MEK1 by cdk5/p35 down-regulates the mitogen-activated protein kinase pathway. *J. Biol. Chem.* **277**, 528-534.

Shea, T. B. (1997). Phospholipids alter tau conformation, phosphorylation, proteolysis, and association with microtubules: implication for tau function under normal and degenerative conditions. *J. Neurosci. Res.* **50**, 114-122.

Shea, T. B. and Beermann, M. L. (1994). Sequential requirements for NFs, MTs, and the MT-associated proteins MAP1B and tau in axonal neurite initiation, elongation and stabilization. *Mol. Cell. Biol.* **5**, 863-875.

Shea, T. B. and Flanagan, L. (2001). Kinesin, dynein and neurofilament transport. *Trends Neurosci.* **24**, 644-648.

Shea, T. B. and Yabe, J. T. (2000). Occam's razor slices through the mysteries of neurofilament axonal transport: can it really be so simple? *Traffic* **1**, 522-523.

Shea, T. B., Sihag, R. K. and Nixon, R. A. (1988). Neurofilament triplet proteins of NB2a/d1 neuroblastoma: posttranslational modification and incorporation into the cytoskeleton during differentiation. *Dev. Brain Res.* **43**, 97-109.

Shea, T. B., Sihag, R. K. and Nixon, R. A. (1990). Dynamics of phosphorylation and assembly of the high molecular weight NF subunit in NB2a/d1 neuroblastoma. *J. Neurochem.* **55**, 1784-1792.

Shea, T. B., Dahl, D., Nixon, R. A. and Fischer, I. (1997). Triton-soluble phosphovariants of the heavy neurofilament subunit in developing and mature mouse central nervous system. *J. Neurosci. Res.* **48**, 515-523.

Shea, T. B., Jung, C. and Pant, H. C. (2003). Does C-terminal phosphorylation regulate neurofilament transport? Re-evaluation of recent data suggests that it does. *Trends Neurosci.* **26**, 397-400.

Shea, T. B., Yabe, J. T., Ortiz, D., Pimenta, A., Loomis, P., Goldman, R. D., Amin, N. and Pant, H. C. (2004). CDK5 regulates axonal transport and phosphorylation of neurofilaments in cultured neurons. *J. Cell Sci.* **117**, 933-941.

Singh, R. P., Dhawan, P., Golden, C., Kapoor, G. S. and Mehta, K. D. (1999). One-way cross-talk between p38(MAPK) and p42/44(MAPK). Inhibition of p38(MAPK) induces low density lipoprotein receptor expression through activation of the p42/44(MAPK) cascade. *J. Biol. Chem.* **274**, 19593-19600.

Stamer, K., Vogel, R., Thies, E., Mandelkow, E. and Mandelkow, E. M. (2002). Tau blocks traffic of organelles, neurofilaments, and APP vesicles in neurons and enhances oxidative stress. *J. Cell Biol.* **156**, 1051-1063.

Sun, D., Leung, C. L. and Liem, R. K. (1996). Phosphorylation of the high molecular weight neurofilament protein (NF-H) by cdk5 and p35. *J. Biol. Chem.* **271**, 14245-14251.

Sun, Q. Y., Wu, G. M., Lai, L., Bonk, A., Cabot, R., Park, K. W., Day, B. N., Prather, R. S. and Schatten, H. (2002). Regulation of mitogen-activated protein kinase phosphorylation, microtubule organization, chromatin behavior, and cell cycle progression by protein phosphatases during pig oocyte maturation and fertilization in vitro. *Biol. Reprod.* **66**, 580-588.

Stone, E. M., Heun, P., Laroche, T., Pillus, L. and Gasser, S. M. (2000). MAP kinase signaling induces nuclear reorganization in budding yeast. *Curr. Biol.* **10**, 373-382.

Tang, B. L. (2003). Inhibitors of neuronal regeneration: mediators and signaling mechanisms. *Neurochem. Int.* **42**, 189-203.

Trinczek, B. A., Ebneth, A., Mandelkow, E. M. and Mandelkow, E. (1999). Tau regulates the attachment/detachment but not the speed of motors in microtubule-dependent transport of single vesicles and organelles. *J. Cell Sci.* **112**, 2355-2367.

Vaillant, A. R., Zanassi, P., Walsh, G. S., Aumont, A., Alonso, A. and Miller, F. D. (2002). Signaling mechanisms underlying reversible, activity-dependent dendrite formation. *Neuron* **34**, 985-998.

Vaudry, D., Stork, P. J., Lazarovici, P. and Eiden, L. E. (2002). Signaling pathways for PC12 cell differentiation: making the right connections. *Science* **296**, 1648-1649.

Veeranna, Amin, N. D., Ahn, N. G., Jaffe, H., Winters, C. A., Grant, P. and Pant, H. C. (1998). Mitogen-activated protein kinases (Erk1, 2) phosphorylate Lys-Ser-Pro (KSP) repeats in neurofilament proteins NF-H and NF-M. *J. Neurosci.* **18**, 4008-4021.

Veeranna, Shetty, K. T., Takahashi, M., Grant, P. and Pant, H. C. (2000). Cdk5 and MAPK are associated with complexes of cytoskeletal proteins in rat brain. *Brain Res.* **76**, 229-236.

Wang, L. and Brown, A. (2001). Rapid intermittent movement of axonal neurofilaments observed by fluorescence photobleaching. *Mol. Biol. Cell* **12**, 3257-3267.

Yabe, J. T., Pimenta, A. and Shea, T. B. (1999). Kinesin-mediated transport of neurofilament protein oligomers in growing axons. *J. Cell Sci.* **112**, 3799-3814.

Yabe, J. T., Jung, C., Chan, W. K.-H. and Shea, T. B. (2000). Phospho-dependent association of neurofilament proteins with kinesin in situ. *Cell Motility Cytoskel.* **42**, 230-240.

Yabe, J. T., Chan, W. K. H., Chylinski, T. M., Lee, S., Pimenta, A. F. and Shea, T. B. (2001a). The predominant form in which neurofilament subunits undergo axonal transport varies during axonal initiation, elongation and maturation. *Cell Motil. Cytoskel.* **48**, 61-83.

Yabe, J. T., Chylinski, T., Wang, F. S., Pimenta, A., Kattar, S. D., Linsley, M. D., Chan, W. K. H. and Shea, T. B. (2001b). Neurofilaments consist of distinct populations that can be distinguished by C-terminal phosphorylation, bundling and axonal transport rate in growing axonal neurites. *J. Neurosci.* **21**, 2195-2205.

Zhang, Y. L., Bing-Sheg, L., Veeranna and Pant, H. C. (2003). Phosphorylation of the head domain of neurofilament protein (NF-M) *J. Biol. Chem.* **278**, 24026-24032.

Zhu, Q., Lindenbaum, M., Levavasseur, F., Jacomy, H. and Julien, J. P. (1998). Disruption of the NF-H gene increases axonal microtubule content and velocity of neurofilament transport, relief of axonopathy resulting from the toxin β'β'-iminodiproprionitrile. *J. Cell Biol.* **143**, 183-193.